Photocatalytic Activity of Heterostructures Based on ZnO and N-Doped ZnO
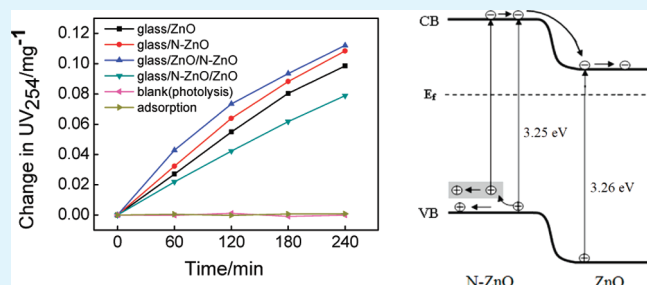
Hongchun Qin,[†,‡] Weiying Li,*[,†] Yujing Xia,[‡] and Tao He*[,‡]

[†]State Key Laboratory of Pollution Control and Resource Reuse, School of Environmental Science and Engineering, Tongji University, Shanghai 200092, China

[‡]National Center for Nanoscience and Technology, Beijing 100190, China

ABSTRACT: Different composite films prepared by coupling ZnO and nitrogen-doped ZnO (N-ZnO) were used to photodegrade humic acids (HA). The catalysts exhibit an activity in the order of glass/ZnO/N-ZnO > glass/N-ZnO >glass/ZnO > glass/N-ZnO/ZnO when light is irradiated from the film to glass substrate. However, glass/ZnO/N-ZnO exhibits a lower activity than glass/N-ZnO/ZnO when light is illuminated from glass to film. Moreover, glass/ZnO/N-ZnO shows a lower activity when light is irradiated from glass to film than that irradiated in the opposite direction. These results suggest that it is not always the case that the presence of a heterojunction at

interface of two semiconductors can definitely result in improving the photoactivity of the heterostructure although it can suppress the recombination of photogenerated charge carriers. They also indicate that photodegradation of HA is mainly via the oxidization by HO• (rather than directly by O_2^- and h^+), which is produced mainly by the reactions with h^+. This implies the importance of fabrication a right heterojunction at the interface between the composite materials when they are used for photocatalysis. We envision that this work will help to develop new photocatalysts, as well as to understand better the photocatalytic mechanism.

KEYWORDS: zinc oxide, heterojunction, hydroxyl radical, photocatalysis, humic acid

INTRODUCTION

Humic acids (HA), one class of humic substances, are natural organic matters formed during the degradation of plant and animal matters. They are complex mixture of many different acids containing carboxyl and phenolate groups. So the molecules can form a supramolecular structure held together by noncovalent forces. HA is widely present in water in the form of small particles. The presence of HA can lead to an undesirable taste and color to drinking water. Such color also makes it unsuitable for the paper, beverage, and textile industries. More important, they are responsible for the formation of disinfection by-products such as haloacetic acids and trihalomethanes upon chlorination,[1] which can cause cancer, carcinogenic, mutagenic, and other toxic effects in human beings.[2,3] Hence, it is critical to remove HA from water. Because the particle size of HA is usually around several hundred nanometers or less, they cannot be removed efficiently by membrane treatment or other conventional water treatment methods (such as precipitation and coagulation). Moreover, they are resistant to biodegradation.

Recently, it has been reported that HA can be degraded into CO_2 or low-molecular-weight carboxylic acids (such as oxalic, formic and acetic) via oxidization by highly reactive oxygen species (such as HO• and O_2^-) produced during photocatalysis.[4−7] Titanium dioxide (TiO_2) and zinc oxide (ZnO) are the most popular photocatalysts used in photodegradation of organic compounds due to their high photoactivity, low cost and non-toxic. To improve the photodegradation of HA, cationic ions (such as calcium and magnesium) have been introduced into

the system since they can enhance the HA adsorption onto catalyst surface.[8,9] To efficiently suppress the recombination of photogenerated charge carriers and, thereby, improve the photocatalytic activity, a semiconductor photocatalyst often combines with another semiconductor so as to build a heterojunction at the interface.[10−13] On the basis of the same idea, mixed-phase anatase—rutile TiO_2 nanoparticles has also been used to photodegrade HA.[14]

Although the presence of a heterojunction at the interface between two semiconductors can lead to suppressing the recombination of photogenerated charge carriers, it cannot guarantee that the photoactivity of the heterostructure can be definitely enhanced since the photoactivity is also closely related to many other factors (such as the irradiation direction and what charge carriers play the major role in the photocatalysis). In this work, we confirmed this argument by preparing some heterostructures with ZnO and nitrogen-doped ZnO (N-ZnO) for photodegradation of HA. As the heterojunction at the interface can facilitate the separation of charge carriers, this can also help to determine what carriers, photogenerated electrons or holes, play a major role in the photocatalysis. We envision that this work will help to develop new photocatalysts for the photodegradation of HA, as well as to understand better the photocatalytic mechanism.

Figure 1. XRD patterns of (a) ZnO and (b) N-ZnO.

Figure 2. XPS spectra of N 1s for N-ZnO. Inset shows N 1s XPS spectrum for ZnO.

■ EXPERIMENTAL SECTION

Preparation of Photocatalysts. All reagents were analytical grade. The urea was used as the doping reagent to prepare nitrogen-doped ZnO (N-ZnO). To prepare the sol used for N-ZnO synthesis, 4.39 g of zinc acetate and 1.20 mL of ethanol amine were first dissolved in 30 mL of ethanol, followed by the addition of a solution containing 1.20 g of urea and 30 mL of ethanol under stirring at 328 K. The resultant mixture was kept at 328 K under stirring until a stable sol was obtained. The sol for ZnO synthesis was prepared by using the same method, but without adding urea.

The glass slide was used as the solid support for all the catalysts, for which the transmittance was ~90% at 360 nm. The glass/ZnO/N-ZnO composite film (heterostructure) was prepared by a spin-coating method. First, a layer of ZnO was prepared on a glass substrate and annealed at 773 K for 0.5 h. Then an N-ZnO layer was prepared atop the ZnO. The films of ZnO, N-ZnO, and glass/N-ZnO/ZnO were prepared by using the same protocol with the corresponding sols, respectively.

Characterization of Photocatalysts. X-ray diffraction (XRD) patterns were collected with a Bruker D8 Focus Diffractometer (Cu Kα, λ = 1.54056 Å). The scanning step was 0.02°. UV−vis absorption spectra were collected in transmission mode using a UV-vis absorption spectrophotometer (Perkin Elmer Lambda 750). The scanning step was 1 nm. The photometric accuracy of the instrument was ±0.01 A for $K_2Cr_2O_7$ standard solution. X-ray photoelectron spectroscopy (XPS) was performed using an ESCALab 250 spectrometer (Thermo Scientific Corp.) with a monochromatic Al Kα X-ray source (1486.6 eV). The Fermi level of XPS instrument was used as the reference for the alignment of energy levels. The binding energy (BE) was calibrated using C1s (284.8 eV) from the adventitious carbon. The energy resolution is ~0.48 eV and the scanning step was 0.1 eV. For the collection of valence band XPS spectra, the scanning step was 0.05 eV.

Photocatalysis of HA. The photocatalyst film was settled in a 200 mL aqueous solution of HA in a sealed reactor. A 500 W Xenon lamp (Beijing Changtuo Technology Co., Ltd.) was used as the light source. The photodegradation of HA was studied in light of the change in UV−vis absorption at 254 nm (UV_{254}) before and after irradiation. All experiments were done at room temperature (26±1 °C).

■ RESULTS

XRD Characterization. Figure 1 shows XRD patterns of ZnO and N-ZnO films. The characteristic peaks corresponding to the diffraction patterns of hexagonal wurtzite phase of ZnO are observed, while no other peak appears. Hence the obtained ZnO and N-ZnO exhibit a wurtzite structure and the introduction of nitrogen does not change the crystal structure of ZnO. The crystal size of N-ZnO (24.0 nm) derived from XRD data[15,16] is
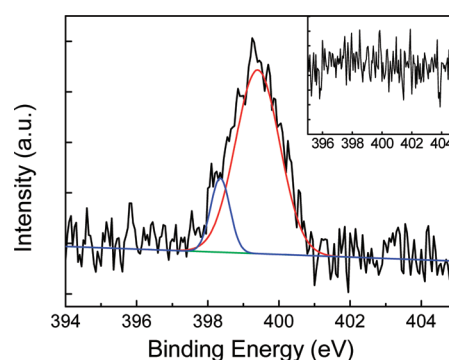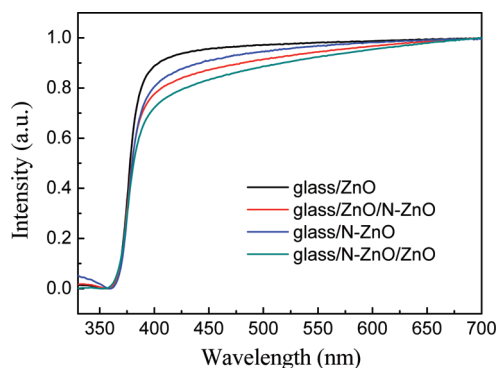

Figure 3. Normalized UV−vis absorption spectra of different samples in transmission mode.

smaller than that of ZnO (30.8 nm). This may be because of the addition of urea during preparation, which behaves as a surfactant that can inhibit the growth of ZnO. It is noted that the intensity ratio of peak (100) to (002) for ZnO is larger than that for N-ZnO, indicating a preferential crystal growth along c axis in N-ZnO. This may be due to the preferential adsorption of urea on different crystal planes.

XPS Spectra. Doping of N in N-ZnO is confirmed by XPS measurements. Figure 2 shows N1s XPS spectra of N-ZnO and ZnO. No peak can be observed for ZnO sample (inset of Figure 2), and two peaks are observed in the spectrum for N-ZnO sample after deconvolution. The BE at ~399.4 eV is attributed to the surface species of N−C and N−N.[17,18] The weak peak at ~398.4 eV is ascribed to the anionic N in O−Zn−N linkage,[17−19] i.e., the doping of N in crystal lattice of ZnO. According to the results of XRD and XPS, therefore, most N exists as surface species, whereas some are doped into ZnO lattice in substitutional mode.

UV−Vis Absorption Spectra. Figure 3 shows the normalized UV-vis absorption spectra of all samples. Pure ZnO only exhibits a strong absorption in the UV region corresponding to the band-to-band transition. Since transmittance of the glass substrate is ~90% at 360 nm, the UV-light absorption by glass can be ignored as the onset edge of band-to-band transition for ZnO is ~380 nm. Compared with ZnO, the samples containing N-ZnO exhibit a small hump at ~450 nm tailing the visible-light region, which is a typical absorption feature of N-doped ZnO. There is almost no change in the optical bandgap upon N doping,
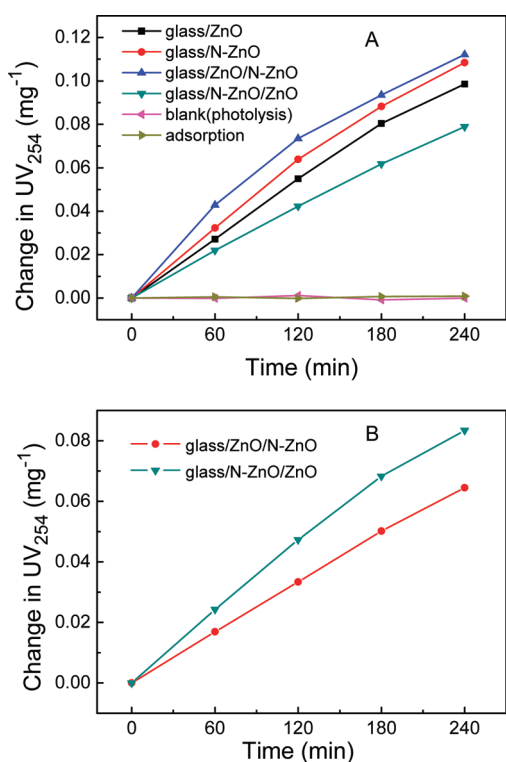
Figure 5. Valence-band XPS spectra of ZnO and N-ZnO.

Figure 4. Change in absorbance caused by per mg catalyst for photodegradation of HA, (A) before and after irradiation from film to glass and (B) before and after irradiation from glass to film.

Table 1. Change in Absorbance before and after Irradiation for Different Samples When Irradiated from Film to Glass for 240 min

sample	mass of film (mg)	change in absorbance	specific photocatalytic activity^c (mg^{-1})
adsorption^a	1.43	0.0012	0.00084
blank^b	0	−0.0001	
glass/ZnO	1.43	0.1409	0.09853
glass/N-ZnO	1.21	0.1312	0.10843
glass/ZnO/N-ZnO	1.32	0.1480	0.11212
glass/N-ZnO/ZnO	1.35	0.1065	0.07889

^{a} Adsorption of glass/ZnO without irradiation. ^{b} Photolysis of HA. ^{c} Change in absorbance of per unit mass catalyst.

which may be due to the amount of N in substitutional mode is not large enough according to the XPS results.

Photocatalysis. The UV$_{254}$ is used to monitor the photodegradation of HA. Figure 4 shows the change of UV$_{254}$ before and after photocatalysis versus irradiation time for different photocatalysts. The results are summarized in Table 1. The specific photocatalytic activity of N-ZnO is 1.10 times that of ZnO, indicating that it exhibits a superior activity to ZnO. This is attributed to doping effects of N, as the introduction of N doping can suppress the recombination of photogenerated charge carriers.[12,20] Moreover, catalysts containing N-ZnO exhibit visible-light response due to the transition from doping levels (possibly N surface species) to conduction band.

It is noted that the heterostructures exhibit different photocatalytic activity under different illumination conditions. The
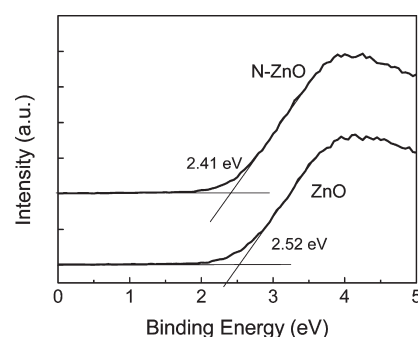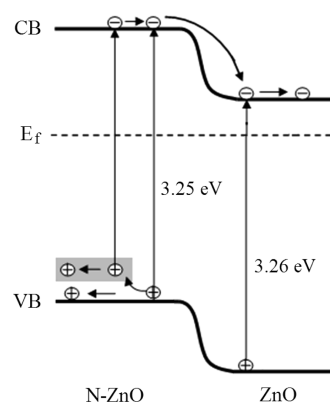

Figure 6. Schematic diagram of energy levels and charge transfer in the composite of ZnO and N-ZnO under irradiation (not to scale). Visible-light response for N-ZnO is also shown in the scheme.
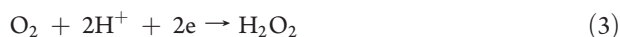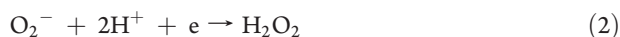
glass/ZnO/N-ZnO composite has the highest activity among all the samples when irradiated from the film to glass, while glass/N-ZnO/ZnO is the lowest. The catalysts exhibit an activity in the order of glass/ZnO/N-ZnO > glass/N-ZnO >glass/ZnO > glass/N-ZnO/ZnO when irradiated from the film to glass (Figure 4A), whereas the glass/N-ZnO/ZnO exhibits a higher photocatalytic activity than glass/ZnO/N-ZnO when irradiated from the glass to film (Figure 4B).

■ DISCUSSION

Determination of Energy Levels. The photocatalytic activity of the heterostructure is closely related to its alignment of energy levels, which is determined by the results of UV−vis absorption spectra and valence-band XPS. The respective bandgap of ZnO and N-ZnO is calculated to be 3.26 and 3.25 eV according to the UV-vis absorption spectra. The BE of onset edge in the valence-band XPS spectrum reveals energy gap between the valence-band maximum and Fermi level (E_{vf}). The respective E_{vf} of ZnO and N-ZnO is determined to be 2.52 and 2.41 eV in light of Figure 5. The Fermi levels are leveled when ZnO is coupled with N-ZnO, leading to the formation of a junction at the interface and, thereby, a built-in electric field across the interface. Alignment of the energy levels in the composite is thus depicted as shown in Figure 6. The photogenerated electrons will accumulate in the ZnO layer and holes accumulate in N-ZnO upon illumination because of the presence of a heterojunction at the interface.

Photocatalytic Mechanism. The photocatalytic activity of a catalyst is determined by the behavior of photogenerated holes

and electrons, which can be produced in ZnO and N-ZnO upon irradiation. The electrons can take part in the reactions shown by eqs 1−4 during the photocatalysis and holes in reactions 5−7. The HA can be photodegraded into CO_2 via reactions 7-9. The recombination of electrons and holes can be suppressed efficiently due to the presence of a heterojunction at the interface of the composite. Furthermore, electrons and holes can arise from both ZnO and N-ZnO. This can explain why glass/ZnO/N-ZnO exhibits the highest activity when light is irradiated from the film to glass, whereas it cannot explain other phenomena.

$$O_2 + e \rightarrow O_2^- \tag{1}$$

$$O_2^- + 2H^+ + e \rightarrow H_2O_2 \tag{2}$$

$$O_2 + 2H^+ + 2e \rightarrow H_2O_2 \tag{3}$$

$$H_2O_2 + e \rightarrow OH^- + HO\bullet \tag{4}$$

$$OH^- + h^+ \rightarrow HO\bullet \tag{5}$$

$$H_2O + h^+ \rightarrow HO\bullet + H^+ \tag{6}$$

$$HA + h^+ \rightarrow CO_2 + H_2O \tag{7}$$

$$HA + O_2^- \rightarrow CO_2 + H_2O \tag{8}$$

$$HA + HO\bullet \rightarrow CO_2 + H_2O \tag{9}$$

The degradation of HA via oxidization by O_2^- (eq 8) is not the major process. Otherwise, when light is illuminated from the film to glass, glass/N-ZnO/ZnO would exhibit a higher activity than ZnO and N-ZnO due to the presence of heterojunction at the interface, accumulation of electrons in ZnO layer and the visible-light response of N-ZnO. No obvious photodegradation of HA is observed when no O_2 is introduced into the reactor. This means that reaction 1 (possibly reactions 2 and 3 as well) plays a key role in the photocatalysis since it can suppress the recombination of charge carriers, and direct oxidation of HA by holes (eq 7) may not be the major degradation process. Thus, the degradation of HA via oxidization by HO• (eq 9) is the major degradation process. The HO• arises mainly from the reactions 5 and 6, instead of from reaction 4. Otherwise, glass/N-ZnO/ZnO would exhibit the highest activity among all the samples. In addition, possibly most electrons participate in the reactions 1-3. When light is irradiated from the film to glass, glass/ZnO/N-ZnO exhibits the highest activity because more HO• (mainly via reactions 5 and 6) can be formed in the outer N-ZnO layer due to the accumulation of holes in it, as well as due to the suppression of recombination and visible-light response of N-ZnO; while glass/N-ZnO/ZnO has the lowest activity since only a few HO• (via reaction 4) can be formed in the outer ZnO layer due to the accumulation of electrons in it and it may be difficult for HA to diffuse into the inner N-ZnO layer.

When light is illuminated from glass to film, only visible light and part UV light can reach the catalysts since the glass can cut off most UV light. So most active species HO• may be caused by the visible light in this case. Visible light can be absorbed by N-ZnO if it first reaches N-ZnO layer instead of ZnO in the composite, whereas most of the visible light can be lost due to the diffuse reflection by ZnO when it first reaches ZnO layer. Thus,

glass/N-ZnO/ZnO exhibits a higher activity than glass/ZnO/N-ZnO when light is illuminated from the glass to film. All these can also explain why glass/ZnO/N-ZnO has a much lower activity when irradiated from the glass to film than that irradiated from the film to glass (Figure 4). It is noted that glass/N-ZnO/ZnO exhibits similar photoactivity when light is irradiated from different sides of the heterostructure. This is possibly because when light is illuminated from glass to film, the absorption of visible light and part UV light by N-ZnO can approximately lead to the formation of equivalent amount of HO• that can take part in HA photodegradation to those when light is illuminated from film to glass because in the latter case most visible light is lost due to the reflection by the outer ZnO layer and most holes accumulates in the inner N-ZnO layer as discussed above.

■ CONCLUSION

Different heterostructures that can be used as photocatalysts were prepared by coupling ZnO and N-ZnO. All the catalysts exhibit an activity in the order of glass/ZnO/N-ZnO > glass/N-ZnO >glass/ZnO > glass/N-ZnO/ZnO when light is irradiated from the film to glass solid support. However, it is noted that glass/N-ZnO/ZnO shows a higher activity than glass/ZnO/N-ZnO when light is irradiated from the glass to film. In addition, the glass/ZnO/N-ZnO exhibits a higher activity when light is irradiated from the film to glass than that when light is irradiated in the opposite direction. All these indicate that HA photodegradation is mainly via the oxidization by HO• rather than directly by O_2^- and h^+. Hence, besides the selected materials and match of energy levels between them, design and fabrication of a right heterojunction at the interface between the composites also play an important role in the photocatalysis.

■ AUTHOR INFORMATION

Corresponding Author

*Fax: +86 21 6598 6313 (W.L.); +86 10 6265 6765 (T.H.). Tel: + +86 21 6598 3869 (W.L.); +86 10 8254 5655 (T.H.). E-mail: liweiying@tongji.edu.cn (W.L.); het@nanoctr.cn (T.H.).

■ REFERENCES

(1) Bekrolet, M.; Uyguner, C. S.; Selcuk, H.; Rizzo, L.; Nikolau, A. D.; Meri, S. *Desalination* **2005**, *176*, 155–166.

(2) Mosteo, R.; Miguel, N.; Martin, C.; Muniesa, S.; Ormad, M. P.; Ovelleiro, J. L. *J. Hazard. Mater.* **2009**, *172*, 661–666.

(3) Liu, S.; Lim, M.; Fabris, R.; Chow, C.; Drikas, M.; Amal, R. *Environ. Sci. Technol.* **2008**, *42*, 6218–6223.

3155

dx.doi.org/10.1021/am200655h |*ACS Appl. Mater. Interfaces* 2011, 3, 3152–3156

(4) Tsimas, E. S.; Tyrovola, K.; Xekoukoulotakis, N. P.; Nikolaidis, N. P.; Diamadopoulos, E.; Mantzavinos, D. *J. Hazard. Mater.* **2009**, *169*, 376–385.

(5) Mariquit, E. G.; Salim, C.; Hinode, H. *Annal. New York Acad. Sci.* **2008**, *1140*, 389–393.

(6) Corin, N.; Backlund, P.; Kulovaara, M. *Chemosphere* **1996**, *33*, 245–255.

(7) Palmer, F. L.; Eggins, B. R.; Coleman, H. M. *J. Photochem. Photobiol. A* **2008**, *148*, 137–143.

(8) Mariquit, E.; Salim, C.; Hinode, H. *J. Chem. Eng. Jpn.* **2009**, *42*, 538–543.

(9) Li, X. Z.; Fan, C. M.; Sun, Y. P. *Chemosphere* **2002**, *48*, 453–460.

(10) Sajjad, A. K. L.; Shamaila, S.; Tian, B.; Chen, F.; Zhang, J. *Appl. Catal., B* **2009**, *91*, 397–405.

(11) Huang, H.; Li, D.; Lin, Q.; Zhang, W.; Shao, Y.; Chen, Y.; Sun, M.; Fu, X. *Environ. Sci. Technol.* **2009**, *43*, 4164–4168.

(12) Cao, Y.Q.; He, T.; Chen, Y. M.; Cao, Y. A. *J. Phys. Chem. C* **2010**, *114*, 3627–3633.

(13) Gao, B.; Ma, Y.; Cao, Y.; Yang, W.; Yao, J. *J. Phys. Chem. B* **2006**, *110*, 14391–14397.

(14) Yigit, Z.; Inan, H. *Water Air Soil Pollut. Focus* **2009**, *9*, 237–243.

(15) Freedsman, J. J.; Kennedy, L. J.; Kumar, R. T.; Sekaran, G.; Vijaya, J. J. *Mater. Res. Bull.* **2010**, *45*, 1481–1486.

(16) Tsay, C. Y.; Cheng, H. C.; Tung, Y. T.; Tuan, W. H.; Lin, C. K. *Thin Solid Films* **2008**, *517*, 1032–1036.

(17) Wang, H.; Ho, H. P.; Xu, J. B. *J. Appl. Phys.* **2008**, *103*, 103704.

(18) Yang, X. Y.; Wolcott, A.; Wang, G. M.; Sobo, A.; Fitzmorris, R. C.; Qian, F.; Zhang, J. Z.; Li, Y. *Nano Lett.* **2009**, *9*, 2331–2336.

(19) Zheng, M.; Wang, Z. S.; Wu, J. Q.; Wang, Q. *J. Nanoparticle Res.* **2010**, *12*, 2211–2219.

(20) Cong, Y.; Zhang, J.; Chen, F.; Anpo, M. *J. Phys. Chem. C* **2007**, *111*, 6976–6982.